J. COMBIN. MATH. COMBIN. COMPUT. 127a (2025) 3557--3572

Journal of Combinatorial Mathematics and Combinatorial Computing
www.combinatorialpress.com/jcmcc

Simulation study on the change of grid node parameters by control command issuance of distributed power access unit

Taofang Xia[1,✉], Chen Gao[1], Yingrong Lin[1], Enguo Zhu[2], Yan Liu[2]

[1] *Marketing Service Center, State Grid Fujian Electric Power Co., LTD., Fuzhou, Fujian, 350000, China*

[2] *China Electric Power Research Institute, Beijing, 100192, China*

ABSTRACT
With the wide application of renewable energy sources, the impact of distributed power access units (DPGUs) on the stability of the power grid is becoming more and more important. This study aims to analyze the impact of DPGU control command issuance on the variation of grid node parameters through simulation. An advanced power system simulation software is used to construct a complex distribution grid model containing multiple DPGUs, including a simulation and analysis method of complex distribution network current characteristics and a voltage hierarchical coordinated control strategy based on inverter regulation for low- and medium-voltage distribution networks, and the process of issuing commands under different control strategies is simulated. By comparing and analyzing the voltage, frequency and power changes of each node before and after the execution of control commands, the specific influence mechanism of DPGU control on grid stability is revealed. The experimental results show that a reasonable control strategy can significantly improve the stability of grid node parameters and reduce fluctuations and mismatches. The results provide a theoretical basis for the optimization of the DPGU control strategy, which is of great significance for realizing the efficient and safe operation of the power grid.

Keywords: current characteristics, inverter regulation, hierarchical coordinated control, simulation analysis, distributed power access unit

1. Introduction

The development of modern society is closely related to the efficient use of electric power, and the electric power industry, which provides efficient electric power for various technical departments, has gradually developed into an economic support and basic industry valued by various countries [1-2]. With the progress and rapid development of China's social and national economy in recent years, China's large-scale electric power system of the power center load continues to grow, in order

✉ Corresponding author.
E-mail address: www23692024@163.com (T. Xia).
Received 03 February 2024; Revised 12 April 2024; Accepted 10 November 2024; Published Online 15 April 2025.
DOI: 10.61091/jcmcc127a-203

to enhance the comprehensive utilization efficiency of the power system, and to ensure the continuous and reliable operation and supply of electricity, in recent years, the Chinese government vigorously develops large-capacity power generation and long-distance centralized transmission, but in this way, the load center and the power generation center. "However, as a result, the load center and generation center do not overlap, and the power often has to be transmitted across long distances to the load location, which seriously affects the voltage stability of the load location [3-6].

At the same time, in recent years, with the serious pollution of the earth's ecological environment and the global renewable energy utilization crisis is becoming increasingly serious, distributed power generation and its related technologies due to the green and clean, high power generation efficiency, flexible layout and other characteristics of the rapid development, and gradually become a new direction of research and development of the power system as well as one of the important issues, so distributed power generation put into operation has brought about two positive factors, the first is that power generation is more decentralized, reducing the number of loads, and thus seriously affecting the voltage stability at the load location [3-6]. Firstly, the power generation is more decentralized, reducing the transmission of power in the network, reducing network losses, and secondly, the SCADA system of distributed power supply is more perfect, making the whole network monitoring and control become more intuitive [7-10]. But can not be ignored is that, after the access of distributed power supply, triggered a huge change in the distribution network structure, from the original single power structure into a multi-source structure. Distributed power grid access to the medium and low voltage distribution network, and thus the operation of the medium and low voltage distribution network static voltage and operational stability also has an impact [11-12]. At present, most of the distributed power supply from the end of the access, will bring a series of problems to the operation of low and medium voltage distribution network such as the quality of power and safety issues, of which the main problems include static voltage, harmonics and other aspects. Therefore, it is undoubtedly very necessary to study the stability of distributed power grid connection [13-15].

Distributed power is a kind of small-scale power system that can supply loads independently. Along with the continuous development of clean energy, the types of distributed power generation are also increasing, which can be divided into renewable and non-renewable according to the different utilization of the initial energy, and can be divided into direct grid-connected power generation and indirect grid-connected power generation through inverters according to the different grid-connected ways of distributed power, and can be divided into solar energy, wind energy, biomass energy, hydropower, tidal energy, geothermal energy, etc., according to the mechanism of generation [16-18].

The traditional distribution network relies on distributed access, which makes it difficult to realize network load balancing, and the uncertainty of the output and load of distributed power sources makes the impact of DG on the power system more serious. The increasing penetration of distributed new energy sources in the power grid has brought a huge impact on the safe and stable operation of the power grid, and in order to improve this problem, it is necessary to reconfigure the distributed power grid framework [19-20].

Aiming at the situation of elevated branch impedance ratio in the power grid, we construct the trend characteristic analysis equations based on the power nodes and load nodes, construct the node injection current-branch current matrix and branch current-node voltage matrix, and design the simulation and analysis method of the trend characteristic of the complex distribution network. The system frequency, voltage and power changes after the power change of a large area power grid system are simulated and analyzed. Subsequently, based on the voltage quality problem caused by distributed power access units, a voltage hierarchical coordinated control strategy for low and medium voltage distribution networks based on inverter regulation is proposed. A simulation model is built on the Matlab/Simulink platform to analyze the output power change and output voltage change of two inverters after adding virtual impedance, and compare the difference between the actual output voltage and the model reference voltage. Finally, taking a 10kV line with high PV penetration as an example, the voltage trend is analyzed by selecting different regulation methods under single-inverter control, multi-inverter control and integrated control, comparing the control results of the traditional strategy and this paper's strategy, and judging whether the proposed medium-low voltage hierarchical coordinated control strategy is able to control the voltage change effectively.

2. Simulation of tidal currents in distributed power access units

In order to adapt to the distributed power supply access distribution grid structure, it is of practical significance to study the complex distribution network trend characteristics of distributed power supply access units (DPGUs). Grid structure trend characterization is a mathematical distribution method as a tool, based on the distribution of power supply and load nodes within the grid structure and voltage and current information as the basis of the electrical analysis method, the trend characterization can be roughly determined by the overall grid structure of the operating state. The simulation analysis of complex distribution network current characteristics of distributed power supply access unit is carried out, and the validity of the current characteristics analysis is verified through experiments.

2.1. Changing tides of access for DPGUs

Fig. 1(a) shows the single power grid structure, and node 1 within this structure is a balanced node, which is the only power node within this grid structure. The arrow shows the direction of the current, and the direction of the current is single-phase. Under the condition that distributed power sources are connected to the grid structure, i.e., as shown in Fig. 1(b), the single-supply grid structure is transformed into a multiple-supply grid structure, and all of the connected distributed power sources, except node 1, also become power nodes within the grid structure, and all of them will inject power into the grid. Based on this, within the multi-power grid structure, the current flows in both directions.

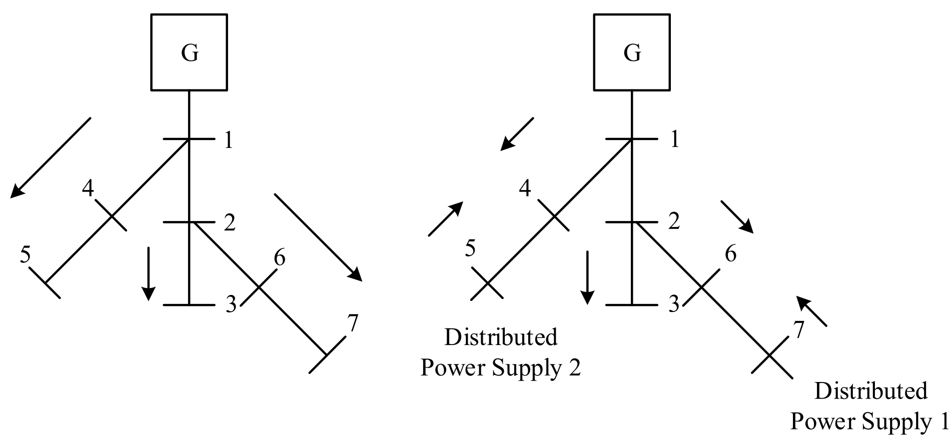

(a) Single power grid structure

(b) The distributed power supply is connected to the grid structure

Fig. 1. Network frame structure

2.2. Trend characterization

2.2.1. Tidal equations. Describe the current injected at the nodes within the three-phase grid in accordance with the node voltage equation of circuit science:

$$I_\eta^j = \sum_{k=1}^{h}\sum_{\tau=a}^{c} A_{\eta\tau}^{jk} = \sum_{k=1}^{h}(A_{\eta a}^{jk}U_a^k + A_{\eta b}^{jk}U_b^k + A_{\eta c}^{jk}U_c^k) \tag{1}$$

Where, h is the total value of the number of nodes within the grid, j,k are the different circuit nodes, τ are the phase voltages, and $A_{\eta\tau}^{jk}$ are the injected currents for the j-node η-phase voltage and the k-node τ-phase voltage.

Introducing Eq. (1) within the power equation enables to obtain:

$$\begin{aligned} P_\eta^{j2} + jQ_\eta^{j2} &= (U_\eta^j \cos\phi_\eta^j + jU_\eta^j \sin\phi_\eta^j) \\ &= \sum_{k=1}^{h}\sum_{\tau=a}^{c}(R_{\eta\tau}^{jk} + jB_{\eta\tau}^{jk})(U_\tau^k\cos\phi_\tau^k + jU_\tau^k\sin\phi_\tau^k) \end{aligned} \tag{2}$$

Where, P_η^j is the j-node η-phase active power, Q_η^j is the j-node η-phase reactive power, U is the branch voltage, ϕ is the phase difference, R is the active power regulation coefficient, and B is the reactive power regulation coefficient. Expanding equation (2) can obtain the node injection power equation of active and reactive power composition of the current characterization equation:

$$\begin{cases} P_\eta^j = U_\eta^j \sum_{k=1}^{h}\sum_{\tau=a}^{c} U_\omega^k (R_{\eta\tau}^{jk}\cos\phi_{\eta\tau}^{jk} + jB_{\eta\tau}^{jk}\sin\phi_{\eta\tau}^{jk}) \\ Q_\eta^j = U_\eta^j \sum_{k=1}^{b}\sum_{\tau=a}^{c} U_\omega^k (R_{\eta\tau}^{jk}\sin\phi_{\eta\tau}^{jk} - jB_{\eta\tau}^{jk}\cos\phi_{\eta\tau}^{jk}) \end{cases} \tag{3}$$

where $\phi_{\eta\tau}^{jk}$ is the phase angle difference between the phase voltage at j node η and the phase voltage at k node τ, $\phi_{\eta\tau}^{jk} = \phi_\eta^j - \phi_\tau^k$.

2.2.2. Direct current algorithm for complex distribution networks. For the three-phase unbalanced islanded grid network structure, the $\eta(\eta = a,b,c)$-phase injection current (I_i^η) at node i is expressed in equation (4):

$$I_i^\eta = \left(\frac{U_i^\eta}{V_i^\eta}\right)^* \tag{4}$$

Where: V_i^n is the modulation factor of node i,η phase and U_i^n is the node i,η phase voltage. The correlation between the node injection current and the tributary currents is determined by Kirchhoff's current law, and describing this correlation in matrix form yields:

$$E^\eta = I_{BIBC}^\eta I^\eta \tag{5}$$

Where: I_{BIBC}^η is the upper triangular constant matrix and I^n is the lower triangular constant matrix. Based on the three-phase unbalanced islanded grid grid structure and Kirchhoff's voltage law can get the correlation between branch currents and node voltages, and describing this correlation in the form of matrices, we get:

$$\Delta W^\eta = I_{BCBV}^\eta E^\eta \tag{6}$$

For the three-phase unbalanced islanded grid structure with fixed topology, I_{BCRV}^η denotes the lower triangular constant matrix. Combining Eq. (5) and Eq. (6) can obtain a generalized matrix expression for direct current characterization of three-phase unbalanced islanded grids, as shown in Eq. (7):

$$\begin{cases} \Delta V^{\eta} = I^{\eta}_{BCBV} I^{\eta}_{BIBC} I^{\eta} = I^{\eta}_{DLF} I^{\eta} \\ I^{\eta}_{DLF} = I^{\eta}_{BCBV} I^{\eta}_{BIBC} \\ W^{\eta} = W^{\eta}_{1} - \Delta W^{\eta} \end{cases} \tag{7}$$

Where: I^{η}_{DIF} is the correlation between node injection current and node voltage.

2.3. Simulation examples

Assuming that all 401 loads corresponding to a province in a large regional grid system have recovery characteristics, 75 generators are equipped with over-excitation limiters and participate in automatic generation control AGC regulation, and setting its 112 transformers as on-load regulator transformer OLTCs, with an action delay of 8~12 s. Under the condition of DC single-loop blocking (loss of 3,000 MW of power) at t=1 s, the analysis of the system frequency as well as some of the node voltages, OLTC stalls, and generator reactive power dynamics in the medium and long term. The calculation example is completed by the direct current simulation method of the complex power grid, with a total simulation time step of 150 and a calculation time of about 80 s. The simulation conditions for this example are CPU=i7-6700@3.4GHz, RAM=4 GB.

Fig. 2 shows the simulation results of a power grid system in a large area, where (a) to (d) are the system frequency change curve, part of the node voltage change curve, part of the on-load regulator transformer ratio change curve and part of the generator reactive power output change curve, respectively. As can be seen from Figs. (a) and (b), after the fault occurs, the system frequency plummets to 49.46 Hz, and the voltage at some nodes also decreases by 0.02~0.08 P.u., and due to the influence of the load recovery characteristics, the voltage still has a tendency to further decrease. As can be seen from Fig. (c), OLTC continuously acts due to the target node voltage continuously lower than the lower limit of its control dead zone until it reaches the control limit, and the tap gear is reduced to 1. As can be seen from Fig. (d), under the influence of the disturbance, part of the generator continuously increases the reactive power output, which increases the motor reactive power by about 50~80 Mvar, and after triggering the OEL, it loses the voltage support, which results in the node voltage dropping as shown in Fig. (b). Voltage dips.

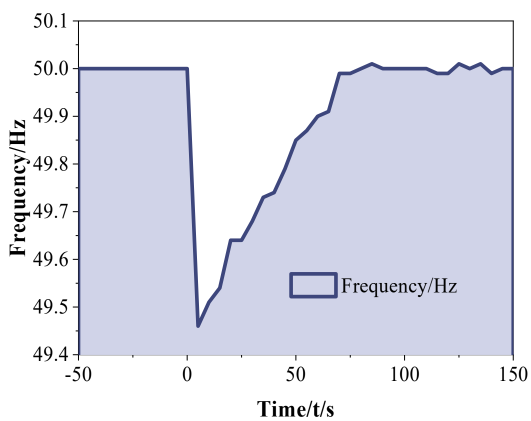

(a) System frequency changes

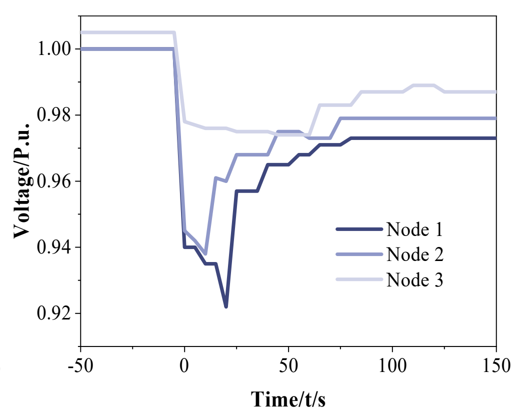

(b) Partial node voltage changes

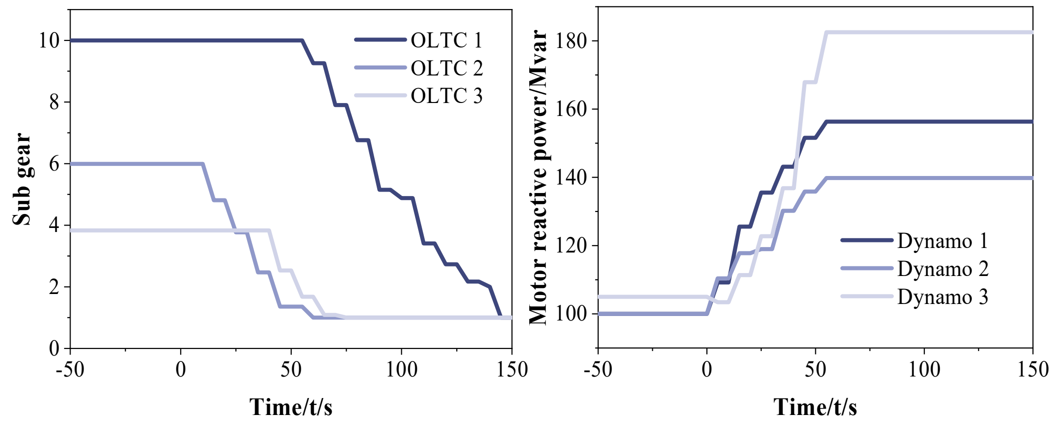

(c) some OLTC changes (d) No work force changes in some generators

Fig. 2. Simulation results of a large area grid system

3. Distribution network control strategy based on inverter regulation

High-percentage PV grid-connection has a significant impact on the distribution network, so the study of the distribution network voltage control under high-percentage PV access and the reduction of the adverse impacts of PV access have become one of the key issues to be solved.

3.1. PV inverter based voltage control methods

This thesis proposes a PV zonal control strategy that can regulate the inverter parameters according to the process when the threshold is exceeded, realizing the in situ regulation of the voltage, which is applicable to both MV and LV PV inverters.

The control area is divided into five zones, of which: U_{Ll} is the lower limit of system voltage operation, U_{L0} is the lower limit of system optimal operation voltage, U_{U0} is the upper limit of system optimal operation voltage, and U_{U1} is the upper limit of system optimal operation. When the voltage at the grid point is $U \leq U_{Ll}$, the III zone control strategy is adopted, at which time the distributed power supply has reached the maximum voltage regulation capability, and regulation cannot be realized by the distributed power supply alone. When $U_{Ll} < U \leq U_{L0}$, zone II control is adopted, and the inverter reactive power output is calculated according to the $Q(U)$ sag curve. When $U_{L0} < U \leq U_{U0}$, it is located in zone I. At this time, the voltage has reached the optimum, and there is no need to regulate the voltage. When $U_{U0} < U < U_{Ul}$, it adopts IV zone control, prioritizing the use of reactive power for voltage regulation according to the $Q(U)$ sag curve, and then utilizing active power for voltage regulation when the reactive power fails to meet the voltage regulation requirements. When $U \geq U_{Ul}$, it is located in V zone, when the voltage at the grid point is too high and the PV is off-grid.

3.2. Medium and low voltage two-stage hierarchical coordinated control strategy

3.2.1. Layered Control Architecture for Low and Medium Voltage. This paper proposes a 2-stage hierarchical coordinated control architecture of "medium voltage first, then low voltage, and medium and low voltage interactive regulation" in the study of medium and low voltage coordinated control strategies for active distribution networks.

3.2.2. Optimization model for low and medium voltage distribution networks:
1) Objective function. The overall control objectives of the medium and low-voltage distribution network are to minimize the distribution network network loss P_{loss}, minimize the voltage deviation rate Up at each node, and maximize the distributed power output P_{DG}, i.e:

$$\begin{cases} \min P_{bose} = \min \sum_{i=1}^{N} (U_i^2 + U_j^2 - 2U_i U_j \cos\theta_{ij}) g_{ij} \\ \min U_D = \min \sum_{ieN_{MV}} \frac{(U_i - U_N)^2}{(U_{\max} - U_{\min})^2} \\ \max P_{DG} = \max \sum_{i=1}^{n} P_{DG,i} \end{cases} \tag{8}$$

Where: i, j indicates the line start and end nodes respectively, N indicates the number of system nodes, U_i, U_j indicates the line start and end voltages respectively, $cos\theta_{ij}$ indicates the phase angle cosine of the node voltages, g_i indicates the line conductance, U_N indicates the node voltage ratings, $U_{\max}, U_{\min}$ indicates the maximum and minimum node voltages, N_{Mv} indicates all the nodes of the medium- and low-voltage distribution network, n indicates the number of distributed power sources, 10 indicates the distributed power sources connected to the nodes, and P_{DGi} indicates the distributed power source connected to the node i. PV grid-connected active power.

In order to facilitate the subsequent solution analysis, the above three objective functions are assigned respectively, and a comprehensive objective function is formed:

$$f = w_1 P_{bss}^* + w_2 U_D^* - w_3 P_{DG}^* \tag{9}$$

Where: f for the integrated objective function, P_{loss}^* for the network loss objective function of the Mississippi value, U_o^* for the node voltage deviation objective function of the Mississippi value, P_{pG}^* for the MV distribution network distributed power consumption objective function of the Mississippi value, the Mississippi value of the benchmark value selected for the initial state of the index value, w_1—w_3 for the weight of each sub-objective can be based on the optimization objectives of the region of the actual control of low-voltage distribution network to determine the demand, and $w_1 + w_2 + w_3 = 1$.

2) Constraints. The control constraints of the medium and low voltage distribution network mainly include the tidal current constraint, branch current constraint, node voltage constraint, node PV output constraint, and adjustable low voltage desk area output constraint.

(1) The current balance constraint is:

$$\begin{cases} P_i - U_i \sum_{jei} U_j (G_{ij} \cos\theta_{ij} + B_{ij} \sin\theta_{ij}) + P_{DG.i} = 0 \\ Q_i - U_i \sum_{jei} U_j (G_{ij} \sin\theta_{ij} - B_{ij} \cos\theta_{ij}) = 0 \end{cases} \tag{10}$$

Where: i and j denote the node number, G_{ij} and B_{ij} denote the conductance and conductance values of the line between nodes i and j, respectively, P_i and Q_i denote the node active and reactive power, respectively, U_i and U_j denote the node voltages, and θ_{ij} is the phase difference of the voltages at nodes i and j.

(2) The branch current constraints are:

$$I_{ij.\min} \le I_{ij.\max} \tag{11}$$

Where: I_i is the branch current between nodes i and j, and I_{ij}.min and I_{ij}.max are the minimum and maximum values of allowable through current in branch ij, respectively.

(3) The node voltage constraint is:

$$U_{\min} \le U_i \le U_{\max} \tag{12}$$

(4) PV output constraints are:

$$P_{DG\,j\min} \le P_{DG\,j} \le P_{DG\,i\max} \tag{13}$$

Where: $P_{DGi\min}$ and $P_{DG.i\max}$ are the minimum and maximum values of the distributed PV output connected at node i, respectively.

(5) The adjustable LV station output constraint is:

$$P_{i.\min} \le P_i \le P_{i.\max} \tag{14}$$

Where: $P_{i.\min}$ and $P_{i.\max}$ are the minimum and maximum values of the output of the adjustable LV station connected to node i, respectively.

3.2.3. Layered control process. The specific steps of the hierarchical control process for medium and low voltage distribution networks are as follows:

1) Determine the regulation time scale for centralized control of the medium-voltage distribution network T.

2) Obtain the load parameters of each node of the medium-voltage distribution network, as well as the parameters of the regulation object.

3) Construct the centralized control model of the MV distribution grid.

4) Solve the mathematical model consisting of Eq. (8)-Eq. (14) using the 2nd-order cone planning algorithm.

5) The regulation power command obtained from the solution is sent to the adjustable low-voltage station area, and the low-voltage station area control is initiated. The specific control process is:

(1) Initial time $t = t_0$ on the LV side to determine the LV station regulation time scale Δt.

(2) Obtain data from each node of the LV distribution network, including parameters such as distribution substation taps, distributed PV, and loads.

(3) Establish the LV station area control model.

(4) Optimize and solve the model based on the inverter control mode of PV plant and adjustable variables such as capacitor bank casting and switching.

(5) Based on the solution result, determine whether the demand of the power regulation command of the MV distribution network is satisfied: if yes, feedback the output power to the MV distribution network in response to the power command. If not, then make $t = t + 1$ and go to the next control process. At the same time, if the solution result meets the demand of the power regulation instruction of the MV distribution network, further determine whether the regulation time of the LV distribution network $t_0 + T$ is reached: if yes, calculate the range of the LV distribution network that can be regulated and feedback to step (2). If not, make $t = t + 1$ and proceed to the next control process.

6) Based on the response power of the LV station, the MV distribution network completes the power regulation under the T time scale window and ends.

3.3. Simulation Analysis

In order to verify the effectiveness of the layered coordinated control strategy for distribution network based on inverter regulation proposed in this paper, a simulation model is built in this paper using Matlab/Simulink simulation platform. The inverter regulation design proposed in this paper is set up in the parallel operation of two inverters based on the hierarchical coordinated control strategy of distribution network. The specific experimental process is to run two inverters in parallel at the initial moment, to access a set of three-phase resistive-inductive loads at 0.05s, and to access a set of three-phase resistive-inductive loads at 0.3s, and the specific experimental results are as follows.

The output power of inverter 1 and inverter 2 are shown in Fig. 3 and Fig. 4, respectively. At 0.05s to 0.3s, both inverter 1 and inverter 2 output active power is 1454.31W, and output reactive power is 1226.4Var. At 0.3s to 0.5s, both inverter 1 and inverter 2 output active power is 2803.36W, and output reactive power is 2210.22Var. Therefore, the proposed inverter regulation-based distribution network hierarchical coordinated control strategy can achieve the purpose of improving the power decoupling accuracy when the inverters are operated in parallel.

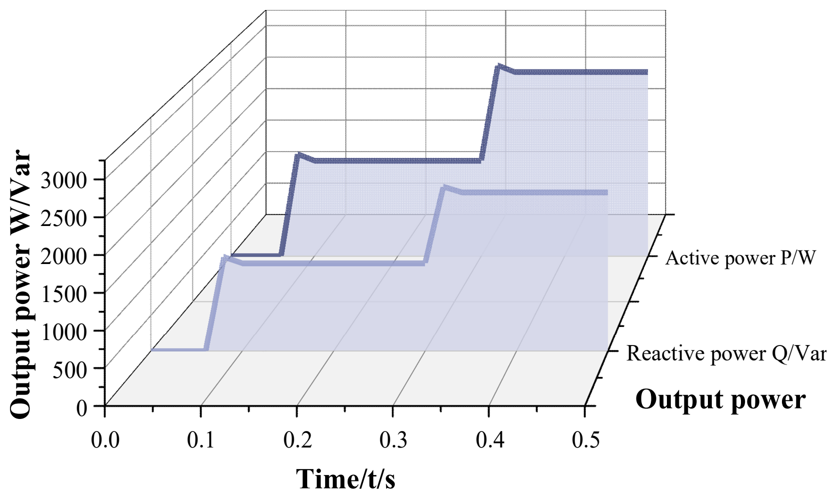

Fig. 3. The output power of the inverter 1

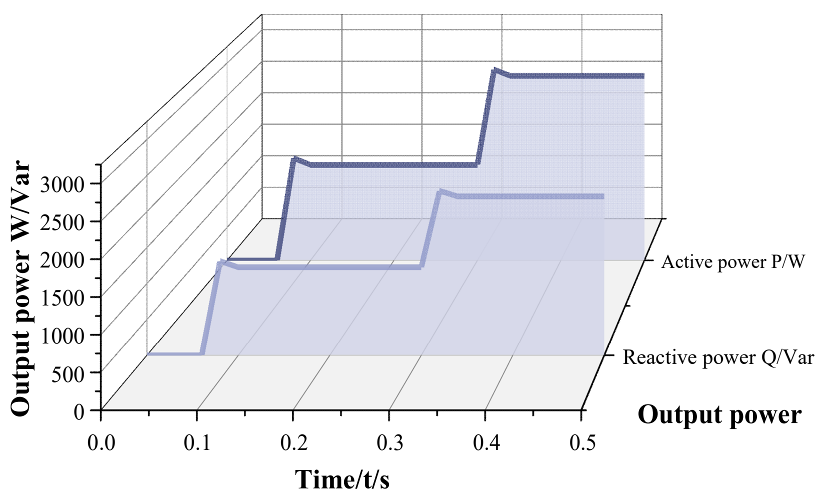

Fig. 4. The output power of the inverter 2

The output voltages of inverter 1 and inverter 2 are shown in Fig. 5 and Fig. 6. The output voltage waveforms of inverter 1 and inverter 2 are good with no voltage drop. At the same time, the output voltage of the controller is shown in Fig. 7, the controller output voltage command is smooth and can completely match the reference model output command voltage, the reference output voltage and the actual output voltage are both 300V, and the error between the output command voltage of the adjustable system and the output command voltage of the reference model is always 0, which proves that the above shunt inverter control system has good control performance.

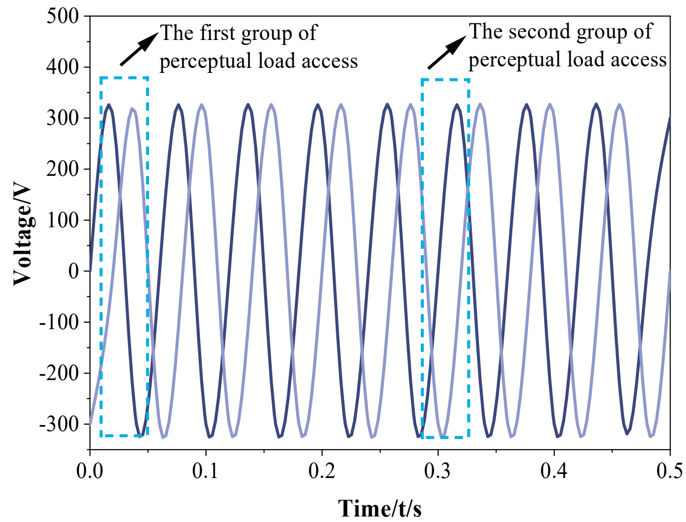

Fig. 5. The output voltage of the inverter 1

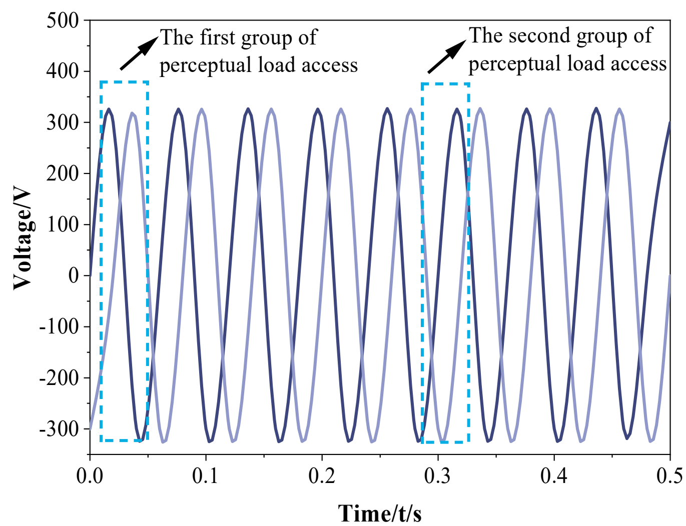

Fig. 6. The output voltage of the inverter 2

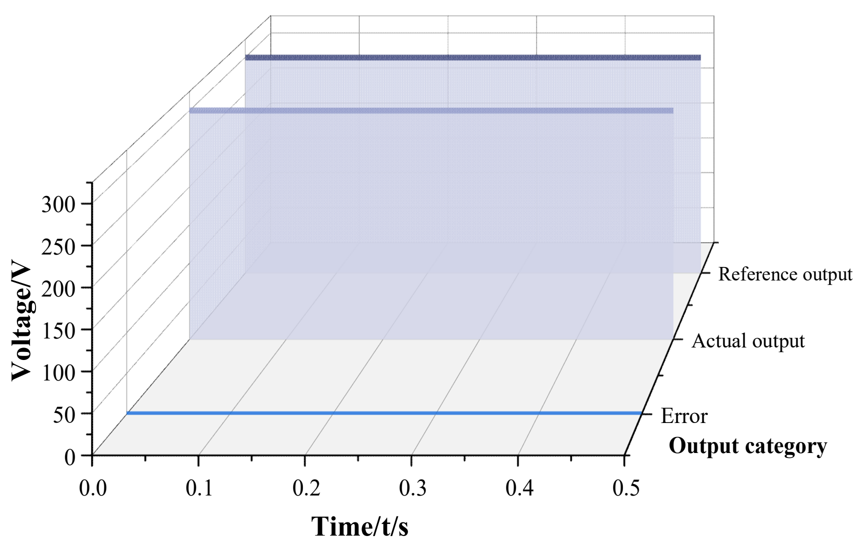

Fig. 7. The output voltage of the controller

4. Analytical validation of algorithms

4.1. Introduction to the algorithm

A 10kV line containing high PV penetration in a certain place is selected to validate the proposed hierarchical coordinated control strategy for distribution network based on inverter regulation based on simulink under Matlab R2018a environment.

The topology of the 10kV line at this location is shown in Fig. 8, the total installed capacity of the line PV is 342kW, there are two forms of household PV and collective PV, and the nodes connected by the PV are controllable. Under normal operation, the bus voltage U0 is 1.05 pu. In the distribution network, the voltage crossing point is generally the PV integration point. In high penetration scenarios, the PV inverter can operate below the unit power factor. For the safe operation of the distribution network, the voltage deviation is set to ±7% of the nominal value according to GB/T 12325-2008 Power Quality Supply Voltage Deviation. The site is a pro-poor PV demonstration area, and the lower limit of the active output of the inverter is set to 80% of its capacity to ensure the economic benefit of users. Based on the voltage history data, the voltage exceeding the upper limit occurs at nodes 5, 6, 13, 18, 21, 22, and 24, where all except node 5 are PV integration points.

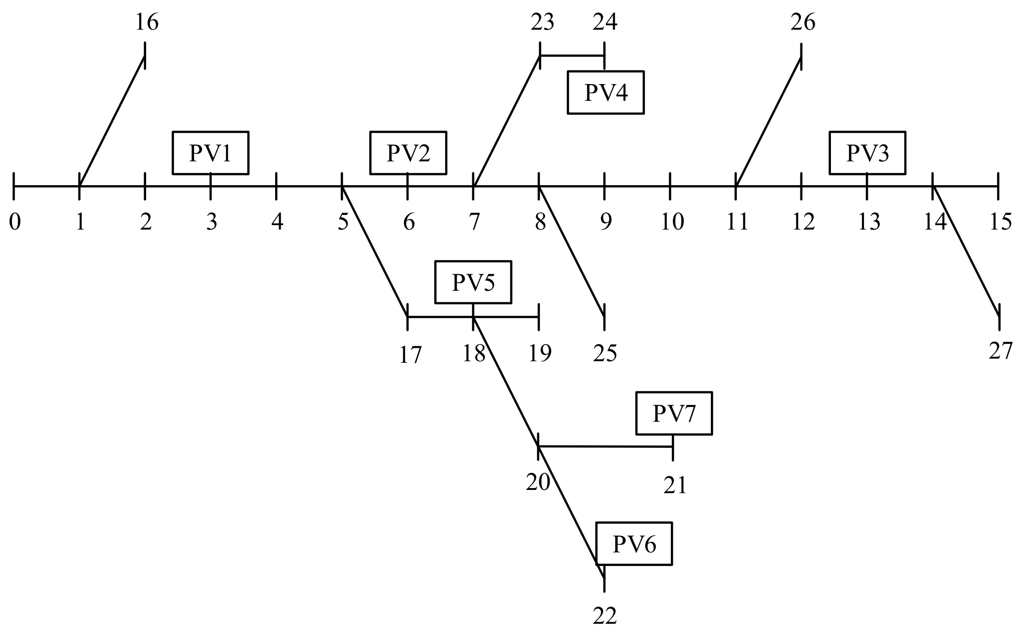

Fig. 8. Topological structure of a 10kV line

4.2. Effectiveness analysis

1) Analysis of single inverter control effectiveness. The voltage control demand of nodes 6, 13, 18, 21 and 24 can be satisfied by single inverter control. The setup scenario: t=0-120s, the voltage is in the safe region, t=120-180s, increasing the light intensity makes the voltage rise continuously, t=180s, the light intensity is restored to the initial setting.

The single inverter control results are shown in Fig. 9. t=140s, due to the light enhancement, the voltage starts to trend up and maintains a high voltage change rate. t=200s around, the node voltages all reach 1.14pu, and the voltage change rate is still positive. t=225s later, the voltage change rate suppression effect is significant, and the voltage distribution curve starts to become “convex” Around t=250s, the voltage growth rate tends to be negative, and the voltage at each node starts to decrease. t=325s, the voltage change rate suppression effect is weakened, and the voltage distribution curve starts to become “concave”. t=350s, the voltage value is lower than 1.08 pu.

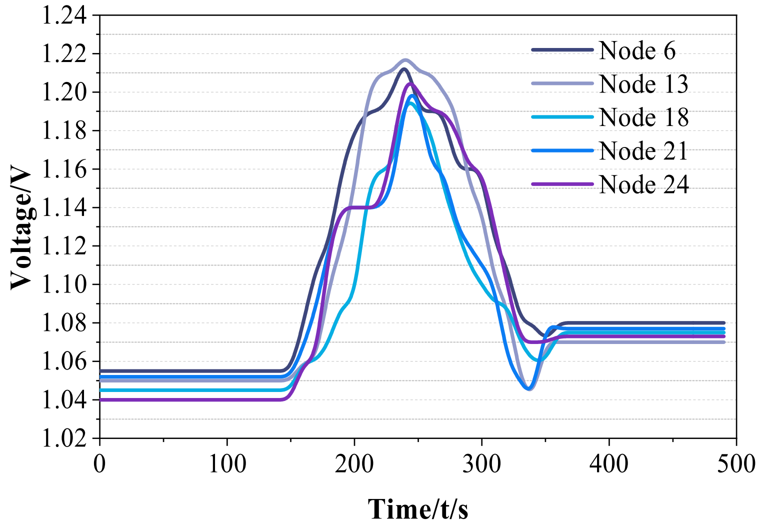

Fig. 9. Single inverter control results

2) Multi-inverter control effectiveness analysis. Node 5 in the line voltage overrun is serious and non-PV integration point, the voltage control generally needs multi-inverter coordinated control. The same as the single-inverter control effectiveness analysis of the scene settings, respectively, using three kinds of control methods:

Mode 1: low voltage control strategy

Mode 2: Medium voltage control strategy

Way 3: medium and low voltage hierarchical control strategy

The control results of multiple inverters are shown in Fig. 10. t=120s, due to the light enhancement, the voltage starts to trend up and maintains a high rate of voltage change, and the voltage reaches 1.082pu at about 150s, and the average value of the rate of voltage change reaches 0.0015pu/s, which reaches the maximum value specified in the arithmetic example. t=150s after the inverters start to control, and the following conclusions can be drawn from Fig. 10:

(1) Mode 1 and mode 2 can not complete the control, but can effectively inhibit the voltage change, and mode 2 inhibition effect is better, with the voltage reaches 1.17pu as the boundary, mode 1 can be delayed for 40s, mode 2 can be delayed for 70s.

(2) Mode 3 can effectively suppress the voltage change when the voltage changes abruptly and finally complete the voltage control, which reflects the effectiveness and superiority of the medium and low voltage hierarchical control strategy in coping with the more serious voltage overrun problem.

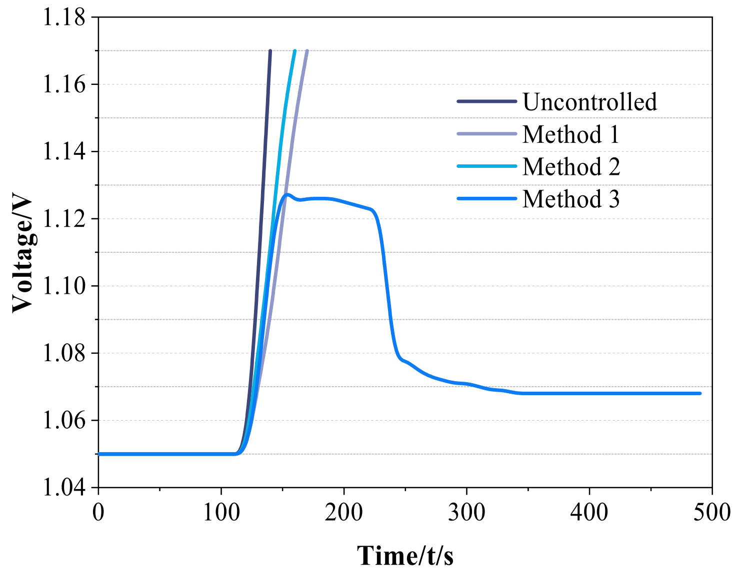

Fig. 10. Multiple inverters control results

4.3. Integrated control analysis

Node 22 in the line is a PV poverty alleviation station area, the PV access capacity is large, and in order to ensure the user's income, the inverter at node 22 is involved in the voltage control of the active injection is limited, the risk of sudden voltage change is large, so the voltage control at node 22 is often a comprehensive control process. Setting scenario: set the light intensity at t=0-70s to make the inverter run in the maximum power point tracking (MPPT) mode. t=70-120s, increase the light intensity setting, and restore the MPPT mode setting at t=120s. t=140-180s, increase the light intensity setting again, and restore the MPPT mode setting at t=180s. t=300-350s, increase the light intensity setting again, and restore the MPPT mode setting at t=350s. t=350s, increase the light intensity setting again, and restore the MPPT mode setting at t=350s. When t=300-350s, increase the light intensity setting again. t=400s, the light intensity restores the MPPT mode setting. Two strategies are used for control:

Strategy 1: The medium and low voltage hierarchical control strategy proposed in this chapter, focusing on the voltage variation rate.

Strategy 2: The traditional inverter control strategy, ignoring the voltage variation rate.

The results of the integrated control analysis are shown in Fig. 11. At t=70s, due to the enhanced light, the voltage starts to rise and maintains a high rate of voltage change. t=120s, the voltage reaches 1.149pu, the control strategy starts to operate, the rate of voltage change is slightly suppressed, and the voltage change curve starts to become convex. t=140s, the rate of voltage change becomes positive again, and the voltage changes again at a higher voltage, and the voltage changes again at a higher voltage, and the voltage changes again at a higher voltage. When t=140s, the voltage change rate becomes positive again, and the voltage rises again with a higher voltage change rate. t=180s, the voltage change rate is obviously suppressed, and the voltage change curve becomes "convex" again. And so on.

In the same scenario, according to the control results of the two control strategies, the following conclusions can be drawn:

1) The trends of the voltage change curves obtained by the two control strategies are basically the same, which further demonstrates the feasibility of the proposed control strategy.

2) Since the traditional inverter control strategy takes the voltage magnitude as the monitoring and control object and ignores the voltage change trend, it leads to a greater delay in the inverter action, while the control strategy proposed in this chapter is controlled through the medium and low

voltage stratification, which participates in the voltage control before the occurrence of voltage overruns and avoids an additional rise in voltage.

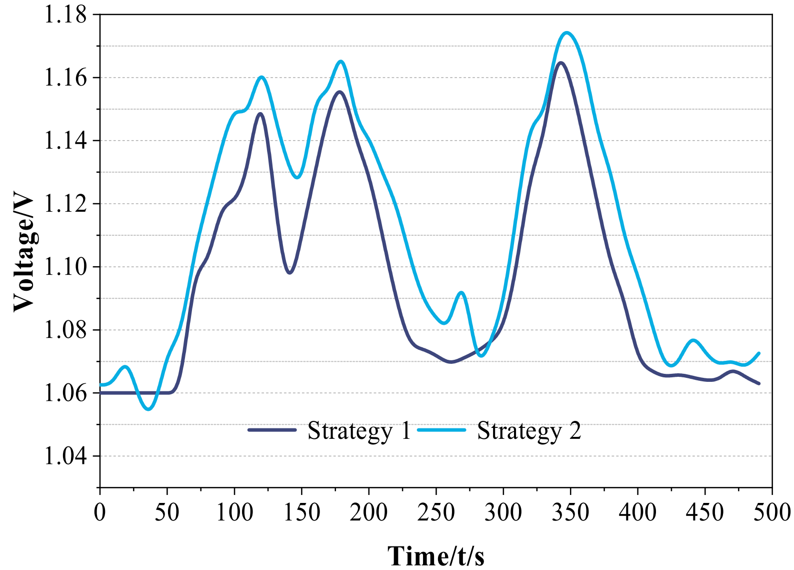

Fig. 11. Synthesized control analysis results

5. Conclusion

In this paper, we design a simulation and analysis method for complex distribution network trend characteristics based on distributed power access unit, and on this basis, we propose a voltage hierarchical coordinated control strategy for medium and low voltage distribution network based on photovoltaic inverter regulation. A certain 10kV line containing high PV penetration is taken as an example and analyzed by simulink for the arithmetic example. The main research results are as follows:

1) Using the tidal current characterization method to analyze the effect of 3000MW power loss on system frequency, voltage and power in a large area grid system, the voltage drops by 0.02~0.08P.u., and the useless power of motor increases by 50~80Mvar. It is shown that the proposed method can analyze the tidal current characteristics of the complex distribution network more accurately in the case of the access of distributed power supply.

2) After the introduction of virtual impedance in the proposed inverter regulation strategy, the inverter power can be equally divided, and the output voltage waveforms of the two inverters are stable, and the error between the reference output voltage and the actual output voltage is 0, which demonstrates the good control effect of the distribution network control strategy based on inverter regulation.

3) In different nodes of the sample line, single-inverter control, multi-inverter control and integrated control experiments are carried out, and the proposed inverter regulation strategy can regulate the voltage in time. The trend of this paper's strategy regulation curve and the traditional strategy regulation curve in the integrated control is close to each other, which verifies the effectiveness of this paper's inverter regulation strategy.

This paper carries out research on grid regulation under the control of distributed power access unit, and has achieved certain results, but there are some shortcomings, and it needs to be explored in depth in the aspects of control accuracy improvement, control delay consideration and coordination of multiple types of equipment.

Funding

This research was supported by the science and technology project of State Grid Co., Ltd.: Research and application of key technologies of low-voltage distributed optical storage and charging acquisition, monitoring and fault isolation (No.: 5700-202455278A-1-1-ZN).

References

[1] Huang, R., Fan, R., Daily, J., Fisher, A., & Fuller, J. (2017). Open‐source framework for power system transmission and distribution dynamics co‐simulation. IET Generation, Transmission & Distribution, 11(12), 3152-3162.

[2] Zhang, X., Bao, J., Wang, R., Zheng, C., & Skyllas-Kazacos, M. (2017). Dissipativity based distributed economic model predictive control for residential microgrids with renewable energy generation and battery energy storage. Renewable Energy, 100, 18-34.

[3] Impram, S., Nese, S. V., & Oral, B. (2020). Challenges of renewable energy penetration on power system flexibility: A survey. Energy Strategy Reviews, 31, 100539.

[4] Horowitz, S. H., Phadke, A. G., & Henville, C. F. (2022). Power system relaying. John Wiley & Sons.

[5] Aziz, T., Lin, Z., Waseem, M., & Liu, S. (2021). Review on optimization methodologies in transmission network reconfiguration of power systems for grid resilience. International Transactions on Electrical Energy Systems, 31(3), e12704.

[6] Shangguan, X. C., Zhang, C. K., He, Y., Jin, L., Jiang, L., Spencer, J. W., & Wu, M. (2020). Robust load frequency control for power system considering transmission delay and sampling period. IEEE Transactions on Industrial Informatics, 17(8), 5292-5303.

[7] Ismael, S. M., Aleem, S. H. A., Abdelaziz, A. Y., & Zobaa, A. F. (2019). State-of-the-art of hosting capacity in modern power systems with distributed generation. Renewable energy, 130, 1002-1020.

[8] Rahman, A., Srikumar, V., & Smith, A. D. (2018). Predicting electricity consumption for commercial and residential buildings using deep recurrent neural networks. Applied energy, 212, 372-385.

[9] Willis, H. L. (2018). Distributed power generation: planning and evaluation. Crc Press.

[10] Zhang, C., Wu, J., Zhou, Y., Cheng, M., & Long, C. (2018). Peer-to-Peer energy trading in a Microgrid. Applied energy, 220, 1-12.

[11] Molzahn, D. K., Dörfler, F., Sandberg, H., Low, S. H., Chakrabarti, S., Baldick, R., & Lavaei, J. (2017). A survey of distributed optimization and control algorithms for electric power systems. IEEE Transactions on Smart Grid, 8(6), 2941-2962.

[12] Kersting, W. H. (2018). Distribution system modeling and analysis. In Electric power generation, transmission, and distribution (pp. 26-1). CRC press.

[13] Choudhury, S. (2020). A comprehensive review on issues, investigations, control and protection trends, technical challenges and future directions for Microgrid technology. International Transactions on Electrical Energy Systems, 30(9), e12446.

[14] Kumar, A., Sah, B., Singh, A. R., Deng, Y., He, X., Kumar, P., & Bansal, R. C. (2017). A review of multi criteria decision making (MCDM) towards sustainable renewable energy development. Renewable and sustainable energy reviews, 69, 596-609.

[15] Qing, X., & Niu, Y. (2018). Hourly day-ahead solar irradiance prediction using weather forecasts by LSTM. Energy, 148, 461-468.

[16] Burke, M. J., & Stephens, J. C. (2018). Political power and renewable energy futures: A critical review.

Energy research & social science, 35, 78-93.

[17] Bedi, G., Venayagamoorthy, G. K., Singh, R., Brooks, R. R., & Wang, K. C. (2018). Review of Internet of Things (IoT) in electric power and energy systems. IEEE Internet of Things Journal, 5(2), 847-870.

[18] Gellings, C. W. (2020). The smart grid: enabling energy efficiency and demand response. River Publishers.

[19] Hirsch, A., Parag, Y., & Guerrero, J. (2018). Microgrids: A review of technologies, key drivers, and outstanding issues. Renewable and sustainable Energy reviews, 90, 402-411.

[20] Kroposki, B., Johnson, B., Zhang, Y., Gevorgian, V., Denholm, P., Hodge, B. M., & Hannegan, B. (2017). Achieving a 100% renewable grid: Operating electric power systems with extremely high levels of variable renewable energy. IEEE Power and energy magazine, 15(2), 61-73.